nature neuroscience

Activation of GPCRs modulates quantal size in chromaffin cells through $G_{\beta\gamma}$ and PKC

Xiao-Ke Chen[1,6], Lie-Cheng Wang[1,6], Yang Zhou[1,2], Qian Cai[3], Murali Prakriya[4], Kai-Lai Duan[1,2], Zu-Hang Sheng[3], Christopher Lingle[4] & Zhuan Zhou[1,2,5]

Exocytosis proceeds by either full fusion or 'kiss-and-run' between vesicle and plasma membrane. Switching between these two modes permits the cell to regulate the kinetics and amount of secretion. Here we show that ATP receptor activation reduces secretion downstream from cytosolic Ca^{2+} elevation in rat adrenal chromaffin cells. This reduction is mediated by activation of a pertussis toxin–sensitive $G_{i/o}$ protein, leading to activation of $G_{\beta\gamma}$ subunits, which promote the 'kiss-and-run' mode by reducing the total open time of the fusion pore during a vesicle fusion event. Furthermore, parallel activation of the muscarinic acetylcholine receptor removes the inhibitory effects of ATP on secretion. This is mediated by a G_q pathway through protein kinase C activation. The inhibitory effects of ATP and its reversal by protein kinase C activation are also shared by opioids and somatostatin. Thus, a variety of G protein pathways exist to modulate Ca^{2+}-evoked secretion at specific steps in fusion pore formation.

In neuroendocrine cells, the large dense-core vesicles can fuse to plasma membrane by two alternative modes: full fusion and 'kiss-and-run'. Full fusion occurs when the vesicular and plasma membranes merge and all the contents are released. Kiss-and-run releases vesicle contents through a transient fusion pore[1–4]. The kiss-and-run mechanism allows partial release by limiting the open time of the fusion pore. Both vesicle release probability and the switch between full fusion and kiss-and-run are subject to presynaptic modulation in synaptic transmission or to hormone secretion in neuroendocrine cells. Modulation of vesicle release probability has been intensively investigated. However, little is known about what determines the switch between full fusion and kiss-and-run[3–5].

A major modulatory mechanism of evoked secretion involves modulation of Ca^{2+} channels by G protein–coupled receptors (GPCRs), thereby altering the extent of Ca^{2+} influx available to initiate exocytosis[6,7]. The molecular steps by which G protein activation[8] leads to increases or decreases in Ca^{2+} current are fairly well understood. However, there are also suggestions that steps in the exocytotic process after Ca^{2+} elevation may also be targets for regulation by G proteins. For example, exocytosis in chromaffin cells and hippocampal neurons seems to be favored by activation of protein kinase C (PKC)[9,10], while $GABA_B$ receptor activation inhibits vesicle priming in the synapse calyx of Held[11]. However, at present, our understanding of the mechanisms of G protein–mediated regulation of secretion remains limited.

The adrenal chromaffin cell provides an important model for investigating neurosecretion[3,12,13]. Chromaffin granules, in addition to the principal molecules of catecholamines and ATP, contain several peptides including somatostatin and opioids[14]. Chromaffin cells also express a variety of GPCRs for endogenous transmitters and modulators, including ACh[15], various peptides[16] and ATP[17]. Our results show that ATP (as well as opioids and somatostatin) causes a $G_{i/o}$-mediated inhibition of secretion by a mechanism involving $G_{\beta\gamma}$ subunits that reduce the lifetime of the fusion pore. Furthermore, simultaneous activation of PKC removes the ATP-mediated inhibition of secretion in rat adrenal chromaffin cells (RACCs).

RESULTS

Inhibition of secretion in RACCs by ATP

We examined the hypothesis that activation of a G protein pathway in RACCs inhibits secretion at steps subsequent to the regulation of Ca^{2+} influx. Direct application of 100 μM ATP to RACCs did not induce any current or increase in $[Ca^{2+}]_i$ (data not shown)[18].

We monitored depolarization-induced secretion by a micro–carbon fiber electrode (CFE) (**Fig. 1a**). In the presence of 100 μM ATP, the depolarization-induced secretion was inhibited by 80 ± 12% (10.8 ± 2.2 pC versus 2.3 ± 0.4 pC; $n = 21$, mean ± s.e.m.). In contrast, ATP inhibited the depolarization-induced Ca^{2+} current (I_{Ca}) by only 25 ± 3% (pulse, $n = 9$) and 21 ± 6% (action potential waveform (APW), $n = 11$) (**Fig. 1a**, right; the inhibition of I_{Ca} reversed within 10 s after washout of ATP). Because the relation between secretion and $[Ca^{2+}]_i$ is not linear[19,20], it is not clear whether the roughly threefold larger ATP inhibition of secretion compared with current is exclusively due to the reduced I_{Ca}, or whether other mechanisms downstream of Ca^{2+} contribute as well.

In RACCs, caffeine and muscarine induce Ca^{2+} release from caffeine-sensitive (ryanodine) and IP3-sensitive Ca^{2+} stores, respectively. If ATP

[1]Institute of Neuroscience, Shanghai Institutes for Biological Sciences and Graduate School, Chinese Academy of Sciences, Shanghai 200031, China. [2]Institute of Molecular Medicine, Peking University, Beijing 100871, China. [3]Synaptic Function Unit, National Institute of Neurological Disorders and Stroke, Bethesda, Maryland 20892, USA. [4]Department of Anesthesiology, Washington University, St. Louis, Missouri 63110, USA. [5]State Key Laboratory of Biomembrane Engineering, College of Life Sciences, Peking University, Beijing 100871, China. [6]These authors contributed equally to this work. Correspondence should be addressed to Z.Z. (zzhou@pku.edu.cn).

Published online 21 August 2005; doi:10.1038/nn1529

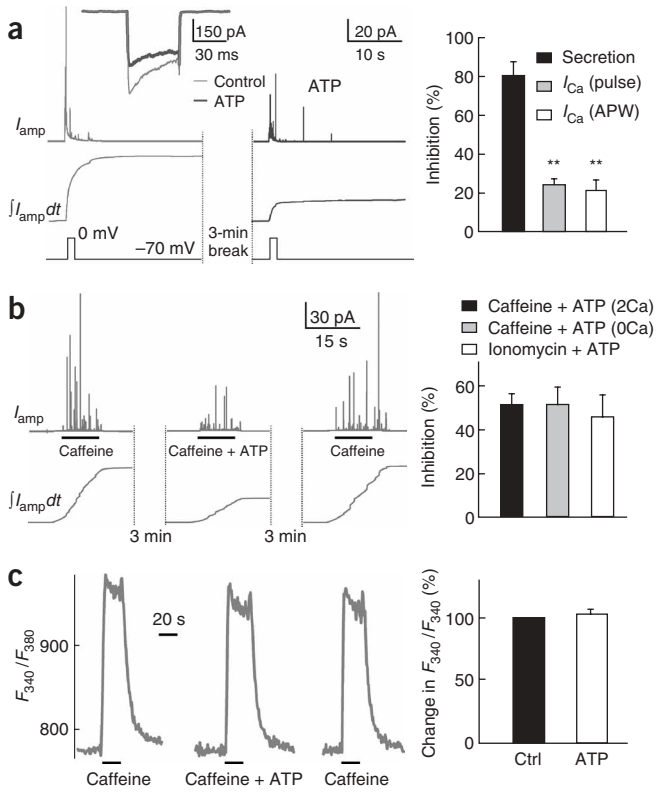

Figure 1 ATP inhibits Ca^{2+}-dependent secretion through multiple signaling pathways. (**a**) ATP inhibits secretion more than I_{Ca}. Left panel shows typical amperometric current traces (I_{amp}, upper trace) and the integrated current signal ($\int I_{amp}dt$) evoked by a 500-ms depolarization in an RACC with or without 100 μM ATP. The right panel summarizes the ATP inhibition of secretion elicited by a 500-ms depolarization, peak I_{Ca} elicited by a step depolarization or by voltage-clamp action potential waveforms (APW). In this and following histograms, the amounts of secretion were evaluated from the integral of the amperometry. Inset at upper left shows the inhibitory effect of ATP on I_{Ca} induced by a 50-ms depolarizing pulse. (**b**) ATP inhibits caffeine-induced amperometric spikes. Left panel shows typical amperometric current traces evoked by caffeine (20 mM for 10 s) co-puffed with or without ATP ($n > 100$). (**c**) ATP has no effect on caffeine-induced $[Ca^{2+}]_i$ elevation.

directly inhibits some step in the secretory process subsequent to Ca^{2+} influx, it would be expected to reduce secretion evoked by Ca^{2+} store mobilization. To test this possibility, caffeine (20 mM) was applied directly to RACCs for 20 s, resulting in a burst of amperometric spikes after a delay of 1–2 s (**Fig. 1b**, left panels). ATP (100 μM, co-puffed with caffeine) inhibited the caffeine-induced amperometric spikes, resulting in a decrease in the integrated amperometric charge or secretion by 52 ± 9% (mean ± s.e.m.) in 2 mM extracellular Ca^{2+} (12.8 ± 2.1 pC in control versus 6.6 ± 0.7 pC in ATP; $n > 100$) and by 50 ± 10% in 0 mM extracellular Ca^{2+} (10.5 ± 2.6 pC in control versus 5.3 ± 1.3 pC in ATP; $n = 7$) (**Fig. 1b**, right). The inhibitory effect of ATP occurred less than 5 s after onset of the application (data not shown). In contrast, ATP had little effect on caffeine-induced intracellular Ca^{2+} transients (103 ± 4% of control, $n = 5$, **Fig. 1c**). This result shows that in addition to inhibiting voltage-dependent Ca^{2+} influx (**Fig. 1a**), ATP inhibits secretion downstream from the elevation of cytosolic Ca^{2+}. Confirming this interpretation, 100 μM ATP also produced a 54 ± 11% reduction (16.5 ± 3.8 pC versus 7.6 ± 2.4 pC; $n = 8$) of the secretion evoked by 10 μM ionomycin (**Fig. 1b**, right), another method of elevating cytosolic Ca^{2+} that bypasses Ca^{2+} channels. ATP had no effect on the ionomycin-induced Ca^{2+} transient (data not shown).

ATP reduces quantal size

The inhibition of caffeine-induced secretion by ATP might reflect either a decreased vesicle release probability or a reduction in total amperometric spike charge (or quantal size). To address this issue, we compared isolated amperometric spikes elicited either by caffeine alone or co-puffed with ATP. Statistically, ATP reduced quantal size, as demonstrated by averaged amperometric spikes and quantal size distribution in the presence or absence of ATP (**Fig. 2a**). On average, ATP had little effect on the number of amperometric spikes induced by caffeine (20 mM for 20 s; 19 ± 3 versus 17 ± 3 amperometric spikes/cell). This suggests that neither the size of the readily releasable pool nor the release probabilities of individual vesicles were changed by ATP.

We also undertook a quantitative analysis of amperometric spike properties. Several features of amperometric spikes reflect important steps in the exocytotic process. Large, rapid amperometric spikes are often preceded by a 'foot', thought to correspond to the initial opening of the fusion pore[2,3,12]. Compared with the control, ATP significantly reduced quantal size by 44 ± 12% (0.54 ± 0.04 pC versus 0.31 ± 0.03 pC) and foot charge by 73 ± 6% (44 ± 4 fC versus 12 ± 2 fC) ($P < 0.01$, **Fig. 2b**). In addition, the half-height duration (HHD) and the foot duration were reduced by 23 ± 7% (6.9 ± 0.6 ms versus 5.2 ± 0.4 ms, $P < 0.05$) and 52 ± 4% (5.4 ± 0.2 ms versus 2.6 ± 0.2 ms, $P < 0.01$), respectively, but ATP had no significant effect on the foot

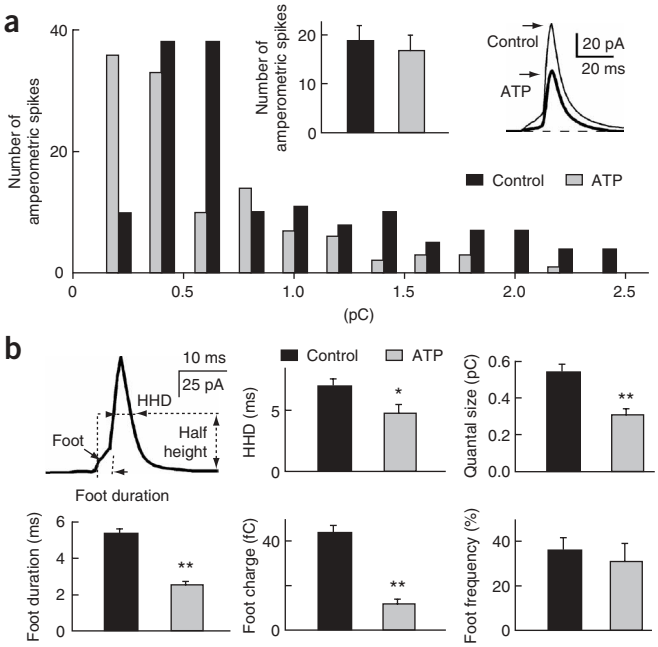

Figure 2 ATP modulates quantal size. (**a**) The distribution of quantal size of caffeine-induced amperometric spikes before and after ATP treatment. Histogram shows the number of amperometric spikes of different quantal size evoked by caffeine (20 mM, 10 s) with or without ATP. Left inset shows the numbers of amperometric spikes elicited by caffeine with ATP ($n = 195$, ten cells) or without ATP ($n = 177$, ten cells). Right inset shows averaged traces (each from 20 amperometric spikes, which were among the fastest 10%; ref. 3) induced by caffeine with or without ATP. (**b**) Quantitative analysis of amperometric spikes induced by caffeine with or without ATP. Data from 12 cells and 329 amperometric spikes that met the 5 s.d. threshold criterion.

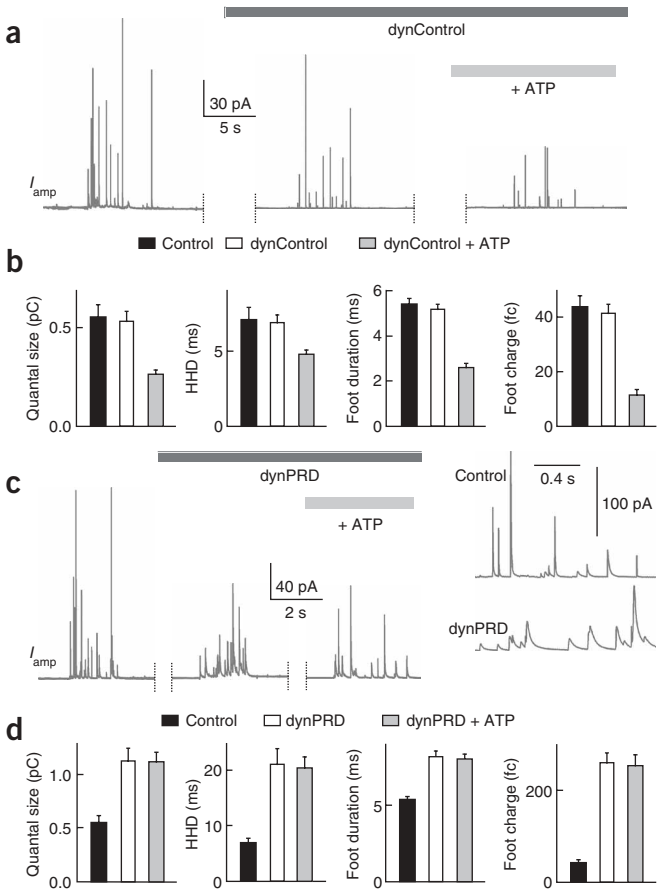

Figure 3 ATP inhibition was eliminated by blocking dynamin function. (**a**) Intracellular dialysis of a scrambled control peptide (dynControl, 0.5 mg/ml, 8–10 min) had no effect on the reduction of quantal size by ATP. (**b**) Statistically, intracellular dialysis of dynControl did not change the ATP effects on quantal size, HHD, foot duration and foot charge. Data from seven cells. (**c**) The mutant dynamin peptide dynPRD eliminated the reduction of quantal size by ATP. A typical I_{amp} trace showed that intracellular dialysis of dynPRD increased quantal size and HHD, and eliminated the reduction of quantal size by ATP. Inset shows the effect of dynPRD on amperometric spikes at expanded time scale. (**d**) Statistically, dynPRD eliminated the ATP effects on quantal size, HHD, foot duration and foot charge. Data from 9 cells.

frequency (36 ± 6% versus 31 ± 8%, **Fig. 2b**). These results demonstrate that ATP does not reduce the vesicle release probability but does reduce quantal size, presumably by reducing the open time of the fusion pore. The dose-response curve for ATP inhibition of quantal size gave an IC_{50} of 115 μM, and a Hill coefficient of 1 (**Supplementary Fig. 1**).

The reduction of both foot duration and HHD suggests that ATP reduces the stability of the fusion pore. If this is the case, manipulations that influence fusion pore stability might alter the ability of ATP to inhibit secretion. For example, dynamin is involved in the pinch-off of endocytosed vesicles[4,21,22] and thus may affect the termination of a release event. Intracellular dialysis of a peptide derived from the proline-rich domain of dynamin (dynPRD, 250 μg/ml), which competitively inhibits endogenous dynamin function[23], increased quantal size, HHD and foot duration dramatically (**Fig. 3**). In the presence of dynPRD, although quantal size, HHD and rise time were increased by 204 ± 18%, 300 ± 36% and 327 ± 24%, the amperometric spike amplitude was reduced by 36 ± 8% (**Fig. 3c,d** and data not shown). In the presence of intracellular dynPRD, quantal sizes were 0.56 ± 0.06 pC (control), 1.14 ± 0.11 pC (dynPRD) and 1.12 ± 0.09 pC (dynPRD + ATP). HHDs were 7.1 ± 0.7 ms (control), 21.3 ± 2.6 ms (dynPRD) and 20.6 ± 1.9 ms (dynPRD + ATP). Foot durations were 5.4 ± 0.2 ms (control), 8.2 ± 0.3 ms (dynPRD) and 8.0 ± 0.3 ms (dynPRD + ATP). Foot charges were 44 ± 4 fC (control), 261 ± 20 fC (dynPRD) and 256 ± 22 fC (dynPRD + ATP). This is consistent with a previous report using anti-dynamin-IgG[4]. Importantly, dynPRD eliminated the ATP inhibition of quantal size, HHD and foot duration (**Fig. 3c,d**). In contrast, intracellular dialysis of a scrambled control peptide (dynControl) was without effect (**Fig. 3a,b**). In the presence of intracellular dynControl, quantal sizes were 0.56 ± 0.06 pC (control), 0.54 ± 0.05 pC (dynControl, 8 min) and 0.27 ± 0.02 pC (dynControl + 100 μM ATP, 10 min). HHDs were 7.1 ± 0.7 ms (control), 6.9 ± 0.5 ms (dynControl) and 4.8 ± 0.3 ms (dynControl + ATP). Foot durations were 5.4 ± 0.2 ms (control), 5.2 ± 0.2 ms (dynControl) and 2.6 ± 0.2 ms (dynControl + ATP). Foot charges were 44 ± 4 fC (control), 42 ± 3 fC (dynControl) and 12 ± 2 fC (dynControl + ATP). Finally, neither dynPRD nor dynControl affected the ATP inhibition of I_{Ca} (data not shown). These results strongly suggest that ATP reduces quantal size by reducing the open time of the fusion pore.

PKC reverses ATP-induced inhibition of secretion

Acetylcholine (ACh) is the endogenous transmitter for chromaffin cells[14]. Activating the muscarinic ACh receptor (mAChR) elevates cytosolic Ca^{2+} (ref. 15) and evokes secretion in RACCs[13]. A 10-s application of 100 μM MCh, a selective mAChR agonist, resulted in a burst of amperometric spikes (**Fig. 4a**, left). Notably, in contrast to the effect of ATP on caffeine- and ionomycin-induced secretion, ATP had little effect on MCh-induced amperometric spikes (**Fig. 4a**, right).

Unlike the steps involved in caffeine- and ionomycin-evoked Ca^{2+} elevations, the mAChR activates a G_q protein that is coupled to a phospholipase C-inositol 1,4,5-trisphosphate (PLC-IP3) pathway[8]. This results in the parallel elevation of cytosolic IP3, leading to release of Ca^{2+} from cytosolic stores and an increase in diacylglycerol, which activates Ca^{2+}-dependent PKC[8]. It therefore seemed possible that the simultaneous activation of PKC by MCh could explain the lack of inhibitory effects of ATP that we observed.

To test this possibility, we examined the ability of bisindolylmaleimide (BIS, 500 nM), a specific membrane-permeant PKC inhibitor, to influence the ATP effects on MCh-induced secretion. In the presence of BIS (**Fig. 4b**), MCh still induced bursts of amperometric spikes, but the response was less, suggesting that the control response to MCh may reflect both the elevation of cytosolic Ca^{2+} and an effect of PKC activation on secretion. When the effect of ATP on MCh-evoked secretion was examined in the presence of BIS, the integrated amperometric spikes were inhibited by 55 ± 11% (**Fig. 4b,d**). In contrast, ATP had no effect on the MCh-induced elevation of cytosolic Ca^{2+} in the presence or absence of BIS (**Fig. 4a**, right, and data not shown). These results suggest that the parallel activation of PKC can reverse the ATP inhibition. Consistent with this idea, in the presence of 5 μM staurosporine (a relatively nonspecific PKC inhibitor), ATP also inhibited MCh-activated secretion (data not shown). Finally, 10 min pretreatment with 200 nM phorbol 12-myristate 13-acetate (PMA), a membrane-permeable agonist for PKC and presynaptic protein Munc13 (refs. 24,25), abolished the ability of ATP to inhibit caffeine-evoked secretion (**Fig. 4c,d**). ATP inhibited 52 ± 9% (12.8 ± 2.1 pC versus 6.6 ± 0.7 pC) of caffeine-induced secretion ($n > 100$), 9 ± 4% (22.1 ± 5.1 pC versus 20.4 ± 5.5 pC) of MCh-induced secretion ($n = 22$) and 55 ± 11% (12.2 ± 2.0 pC versus 5.4 ± 1.3 pC) of MCh-induced secretion when

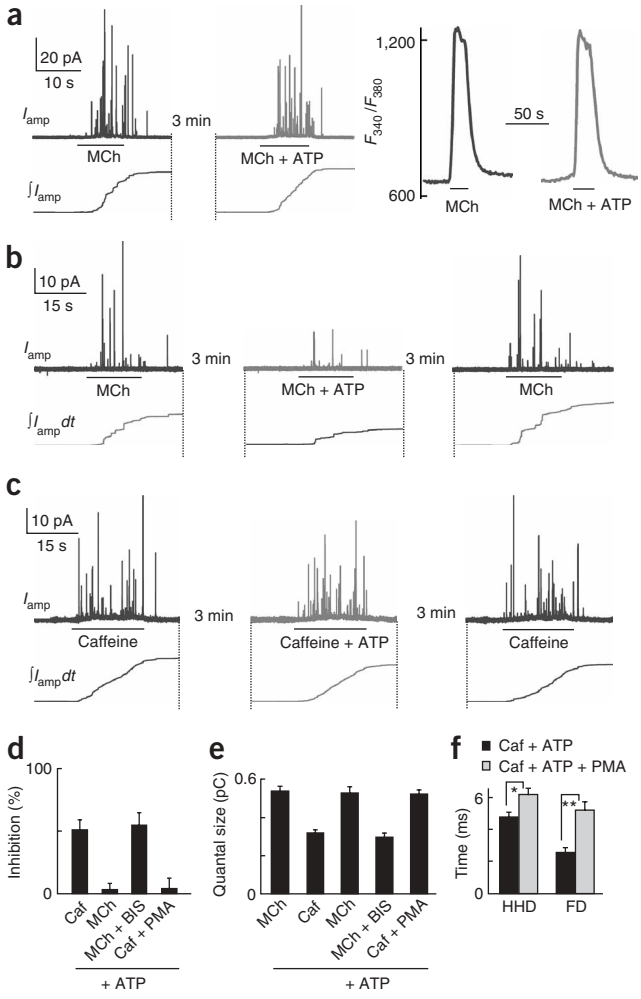

Figure 4 Activation of PKC reverses the ATP-induced inhibition of secretion. (**a**) 100 μM ATP had little inhibitory effect on secretion (left) and $[Ca^{2+}]_i$ elevation (right) elicited by 0.1 mM MCh ($n = 6$). (**b**) In presence of 500 μM BIS, ATP inhibited MCh-induced secretion in a representative cell. (**c**) After pretreatment with 200 nM PMA for 10 min, the inhibitory effects of ATP on caffeine-evoked secretion were eliminated in a representative cell. (**d**) Summary of effects of ATP on secretion evoked by MCh in the absence or presence of BIS. (**e**) Summary of effects of ATP on quantal size evoked by MCh in the absence or presence of BIS and the effects of PMA on reduction of quantal size by ATP. (**f**) PMA eliminated the effects of ATP on the kinetics of amperometric spikes.

cells were pretreated with 500 nM BIS ($n = 8$). ATP inhibited 5 ± 9% (17.1 ± 3.2 pC versus 15.6 ± 2.8 pC) of caffeine-induced secretion when cells were pretreated with PMA ($n = 8$). Taken together, these results suggest that activation of PKC removes the inhibitory effects of ATP on Ca^{2+}-dependent secretion.

Activation of PKC in chromaffin cells directly increases the size of the readily releasable pool[9], essentially enhancing the rate of recruitment of vesicles for secretion[26]. In our experiments, the possibility that PKC eliminated the ATP inhibition by this mechanism could be ruled out, as PKC reversed the ATP effect on both quantal size and amperometric spike kinetics. In bovine chromaffin cells, PMA treatment also reduces the size of digitonin (a non-physiological secretagogou)-induced amperometric spikes[27]. In our experiments, however, PMA treatment had no obvious effect on quantal size of caffeine-induced secretion (**Supplementary Fig. 2**). We found that, like in bovine cells, PMA itself reduced quantal size of digitonin-induced amperometric spikes in rat cells (**Supplementary Fig. 3**). Thus, PMA has no effect on quantal size if the release is induced by physiological stimuli. Analysis of the quantal size of amperometric spikes evoked by MCh showed no difference in the presence or absence of ATP. However, pretreatment with BIS to inhibit PKC restored the ability of ATP to reduce quantal size during MCh-evoked secretion. Consistent with this, pretreatment with PMA eliminated the ATP-induced reduction of quantal size during caffeine-evoked secretion (**Fig. 4e**). ATP inhibited 44 ± 12% (0.54 ± 0.04 pC versus 0.31 ± 0.02 pC) of caffeine-induced quantal size ($n = 12$), 2 ± 2% (0.53 ± 0.03 pC versus 0.53 ± 0.05 pC) of MCh-induced quantal size ($n = 22$), and 45 ± 8% (0.53 ± 0.03 pC versus 0.29 ± 0.03 pC) of MCh-induced quantal size when cells were pretreated with 500 nM BIS ($n = 8$). PMA treatment eliminated the ATP inhibition in quantal size (0.53 ± 0.04 pC versus 0.54 ± 0.04 pC, $n = 8$). PMA also eliminated the ATP-induced changes in amperometric spike kinetics (HHD and foot duration; **Fig. 4f**). Comparing amperometric spikes evoked by caffeine + ATP and caffeine + ATP + PMA, the HHDs were 4.8 ± 0.3 ms versus 6.2 ± 0.4 ms, and the foot durations were 2.6 ± 0.2 ms versus 5.2 ± 0.3 ms ($n = 8$). In addition, like PMA, MCh eliminated the ATP-induced changes in amperometric spike kinetics (data not shown). Although PMA activates both PKC and Munc13 (refs. 24,25), the data from BIS and staurosporine are consistent with the hypothesis that PKC is responsible for the MCh effect on removing the ATP inhibition. We conclude that PKC activation removes the inhibitory effect of ATP on the fusion pore.

ATP mediated effects by P2Y receptor coupled to $G_{i/o}$

Caffeine-evoked secretion was inhibited by only −5 ± 5% by ATP in the presence of reactive blue-2 (RB-2, 30 μM), an antagonist of P2Y purinoceptors (**Fig. 5a**, left, and **Fig. 5b**). The inhibition of caffeine-induced secretion by ATP was sensitive to pertussis toxin (PTX). In cells from the same culture recorded on the same day, the extent of ATP-mediated inhibition was 46 ± 9% (10.4 ± 1.6 pC versus 5.0 ± 2.1 pC, $n = 8$) in controls, but 5 ± 5% (12.4 ± 2.8 pC versus 13.1 ± 1.9 pC, $n = 8$) in RB-2, and −6 ± 4% (11.6 ± 3.3 pC versus 12.1 ± 3.5 pC, $n = 14$) in PTX-treated cells (**Fig. 5a**, right, and **Fig. 5b**). PTX also reversed the ATP-induced inhibition of I_{Ca} in the same batch of cells (data not shown). Thus, the ATP-induced inhibition of secretion is mediated by a PTX-sensitive $G_{i/o}$ signaling pathway.

Although the ATP concentration (100 μM) used in our study is close to the physiological level[28], the relatively high concentration might have had some nonspecific effect on quantal size. To exclude this possibility, we used 2-methylsulfate ATP (2-MeS-ATP; 200 nM), a specific and high-affinity P2Y agonist[18], to confirm that P2Y is responsible for the ATP inhibition of quantal size in RACCs. Indeed, 2-MeS-ATP (200 nM) inhibited quantal size and amperometric spike kinetics to the same extent as did ATP (100 μM) and had no effect on the caffeine-induced $[Ca^{2+}]_i$ transient (**Supplementary Fig. 4**).

We next evaluated whether the pathway underlying the inhibitory effects of ATP on secretion is mediated by α or βγ subunits of the $G_{i/o}$ protein. A primary effector pathway of the activated $G_{i/o}$ α subunit is suppression of the activation of adenylate cyclase, thereby reducing cAMP and minimizing PKA activity[8]. To test the possible involvement of adenylate cyclase in the ATP-mediated effects, cells were preincubated with the cell-permeable cAMP/PKA reagents 8-bromine cAMP, forskolin or H89 for 10–15 min. None of these compounds altered the ATP inhibition of total secretion and quantal size, excluding the involvement of a $G_{i/o}$ α pathway (**Fig. 5c**). After 30 min preincubation

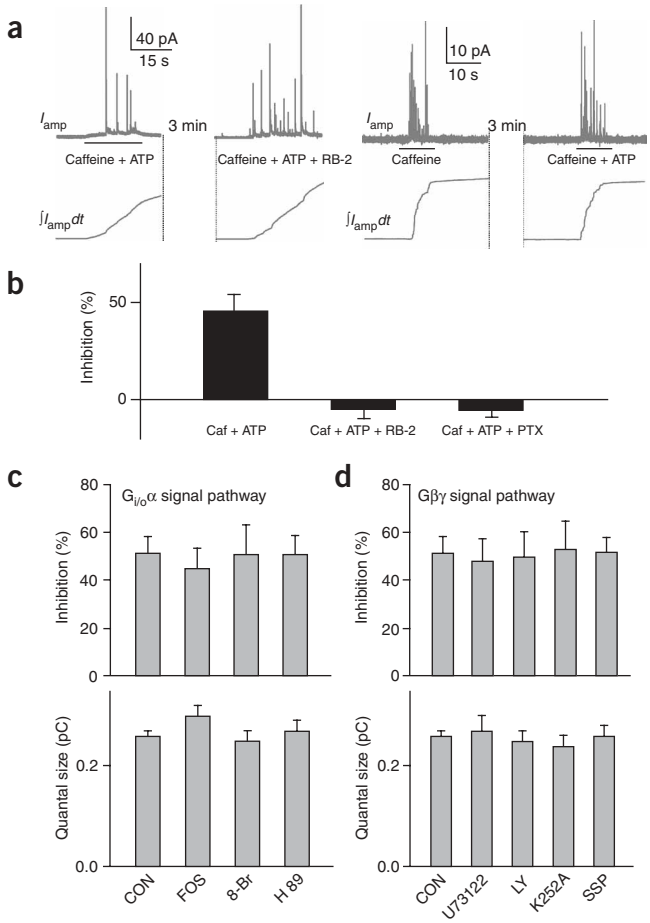

Figure 5 ATP inhibits secretion through activation of a $G_{i/o}$ protein. (**a**) ATP inhibited caffeine-induced secretion through the P2Y receptor by means of a PTX-sensitive $G_{i/o}$ protein. Traces show representative amperometric spike traces induced by caffeine with or without ATP following pretreatment of the cell with 30 μM RB-2 (left) or 250 ng/ml PTX (right) for 24 h. (**b**) Summary of statistical data in **a**. (**c**) The effects of reagents that interfere with cAMP metabolism on the ATP inhibition of caffeine-induced secretion and quantal size. FOS, forskolin. CON, control (applying 0.1 mM ATP only). 8-Br, 8-bromine cAMP. (**d**) The effects of reagents that interfere with $G_{\beta\gamma}$ metabolism on the ATP inhibition of caffeine-induced secretion and quantal size. LY, LY294002. SSP, staurosporine. CON, control (as in **c**).

with forskolin (50 μM, $n = 11$), 8-bromine cAMP (8-Br cAMP, 100 μM, $n = 9$) or H89 (10 μM, $n = 8$), ATP inhibited 45 ± 10% (17.9 ± 4.5 pC versus 9.9 ± 1.8 pC), 48 ± 12% (16.4 ± 3.6 pC versus 8.5 ± 2.2 pC), and 51 ± 10% (11.5 ± 3.6 pC versus 5.4 ± 2.1 pC) of caffeine-induced total secretion, respectively. The corresponding values for quantal size were 0.33 ± 0.03 pC (forskolin), 0.30 ± 0.02 pC (8-Br cAMP) and 0.32 ± 0.02 pC (H89). In **Fig. 5c**,**d**, ATP inhibited 52 ± 6% of total secretion. Quantal size was 0.31 ± 0.02 pC in the presence of ATP (control, $n = 100$).

βγ subunits of the trimeric $G_{i/o}$ protein are known to activate second messenger signaling pathways of adenylate cyclase II, phosphatidylinositol 3-kinase (PI3K), phospholipase C-β2 (PLC-β2), serine/threonine kinases and tyrosine kinases[8,29,30]. We therefore tested the effects of pretreatment with LY294002 for PI3K, U73122 for PLC-β2, staurosporine for serine/threonine kinase and K252A for tyrosine kinase. None of these compounds influenced the ATP inhibition of total secretion and quantal size, excluding the effector pathways listed above from the ATP inhibition (**Fig. 5d**). After preincubation with U73122 (2 μM, puff for 3 min, $n = 8$), LY294002 (40 μM, 30 min, $n = 11$), K252A (20 μM, 30 min, $n = 9$) or staurosporine (5 μM, 15 min, $n = 13$), ATP inhibited 48 ± 12% (9.6 ± 3.5 pC versus 5.0 ± 1.8 pC), 50 ± 13% (10.3 ± 2.4 pC versus 5.1 ± 1.6 pC), 53 ± 14% (10.4 ± 2.8 pC versus 4.7 ± 1.4 pC) and 52 ± 8% (10.2 ± 2.5 pC versus 4.8 ± 0.8 pC) of caffeine-induced secretion, respectively. The corresponding quantal size values were 0.32 ± 0.03 pC (U73122), 0.29 ± 0.02 pC (LY294002), 0.27 ± 0.02 pC (K252A), and 0.31 ± 0.02 pC (staurosporine).

Direct role of $G_{\beta\gamma}$ subunits in inhibition of secretion

We next examined whether $G_{\beta\gamma}$ subunits directly participate in the ATP-mediated inhibition of secretion. We used mSRIK, a membrane-permeable peptide that binds to the $G_{\beta\gamma}$ subunit, to shield the endogenous and activated $G_{\beta\gamma}$ subunits in chromaffin cells[31,32]. After pretreatment with mSRIK (30 μM) for 30 min, ATP was unable to reduce caffeine-induced secretion (**Fig. 6a**,**b**). It was possible that mSRIK occluded the inhibitory effect of ATP by altering the activation of PKC in some way, thereby mimicking the effect of MCh. To exclude this possibility, we tested the effect of 500 nM BIS on the blockade produced by mSRIK, but it was without effect (**Fig. 6b**). After pretreatment with mSRIK, ATP inhibited only 9 ± 3% of the caffeine-induced secretion (12.2 ± 2.6 pC versus 11.2 ± 1.8 pC, $n = 13$), but 500 nM BIS had no effect on the action of mSRIK on the ATP inhibition (11 ± 4%; that is, 12.2 ± 2.6 pC versus 10.4 ± 2.3 pC) of the caffeine-induced secretion ($n = 8$).

To obtain additional evidence that $G_{\beta\gamma}$ subunits directly inhibit secretion in RACCs, we dialyzed purified $G_{\beta1\gamma2}$ subunits[33] through the whole-cell patch pipette. In control cells, there was no significant reduction in secretion evoked by 1 s depolarization at 4-min intervals (**Fig. 6c**, left traces). Whole-cell dialysis of $G_{\beta1\gamma2}$ subunits (0.5 ng/μl) for 4 min reduced depolarization-induced secretion (**Fig. 6c**, right) by reducing quantal size (**Fig. 6d**) by 69 ± 2% (from 0.61 ± 0.04 pC to 0.19 ± 0.02 pC) of control and by reducing I_{Ca} by 22 ± 4% of control ($n = 5$, data not shown). Furthermore, $G_{\beta1\gamma2}$ markedly reduced foot duration by 44 ± 9% (from 5.7 ± 0.7 ms to 3.2 ± 0.2 ms), foot charge by 82% (from 51 ± 6 fC to 9 ± 2 fC) and HHD by 26 ± 8% (from 6.3 ± 0.5 ms to 4.7 ± 0.6 ms) compared with the control, indicating that the fusion pore is directly regulated by $G_{\beta\gamma}$ (**Fig. 6d**, $n = 5$). The effects of $G_{\beta\gamma}$ on quantal size, foot duration and HHD are not due to the reduction of Ca^{2+} currents by $G_{\beta1\gamma2}$, because these effects were also obtained when caffeine or ionomycin, which increase $[Ca^{2+}]_i$ without voltage-gated Ca^{2+} channels, were used to trigger secretion (**Figs. 6e**,**f**). $G_{\beta1\gamma2}$ subunits significantly reduced the evoked secretion, with quantal size dropping from 0.61 ± 0.08 pC to 0.29 ± 0.04 pC, HHD from 6.3 ± 0.8 ms to 4.6 ± 0.6 ms, foot duration from 6.1 ± 1.3 ms to 1.5 ± 0.2 ms and foot charge from 51 ± 9 fC to 7 ± 1 fC ($n = 3$, $P < 0.01$ for all except HHD, for which $P < 0.05$).

ATP and $G_{\beta1\gamma2}$ subunits inhibited both depolarization-activated I_{Ca} and quantal size (**Figs. 1a** and **Fig. 6c**). On average, ATP reduced the number of depolarization-induced amperometric spikes and quantal size by 53 ± 8% and 45 ± 3%, respectively (**Supplementary Fig. 5**). To examine whether the small (22–25%) inhibition of I_{Ca} by ATP or $G_{\beta\gamma}$ was responsible for the reduction of quantal size, cells were depolarized from −70 mV to 0 mV or 30 mV for 0.5 s (**Supplementary Fig. 5**). In these experiments, I_{Ca} and the number of amperometric spikes evoked at 30 mV were 83 ± 5% and 55 ± 12%, respectively, of that at 0 mV, while quantal size was similar at 0 mV and 30 mV. Thus, the reduced quantal size was not due to the inhibition (by 22–25%) of the depolarization-induced Ca^{2+} current by ATP or $G_{\beta\gamma}$ (**Supplementary**

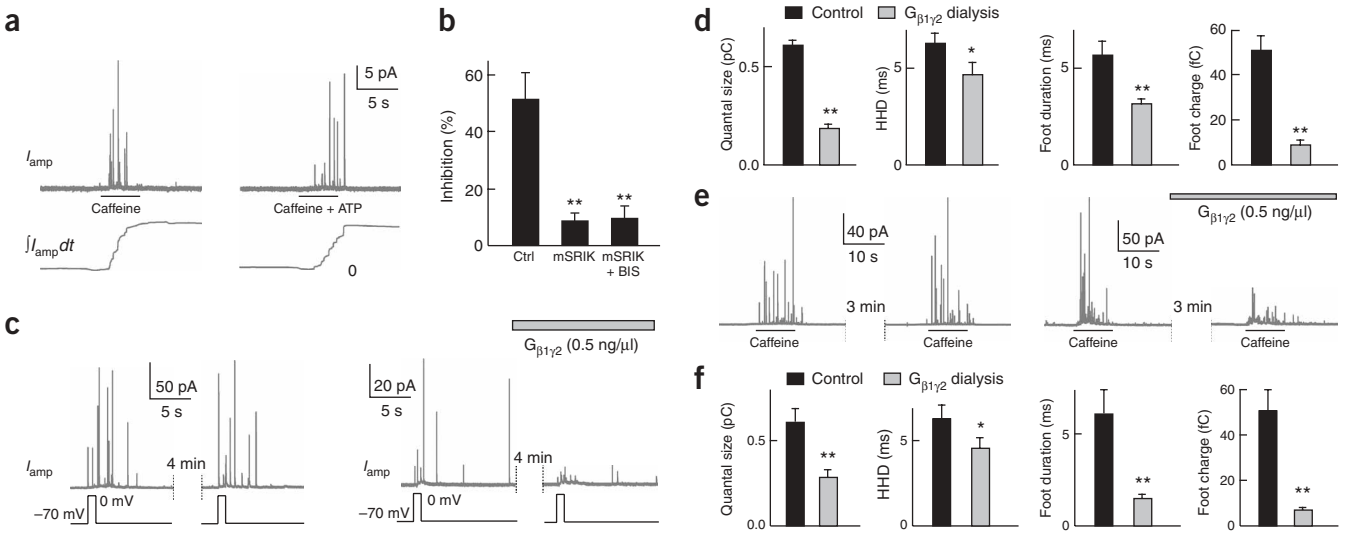

Figure 6 $G_{\beta\gamma}$ subunits mediate the ATP-induced inhibition of secretion. (**a**) In the presence of mSRIK (30 μM, 30 min, 37 °C), the inhibitory effect of ATP on caffeine-induced secretion was reversed in a representative cell. (**b**) Statistics of panel **a**, and the effect of 500 nM BIS on the blockade produced by mSRIK. (**c**) Secretion evoked by 1-s depolarizing pulses to 0 mV was compared for cells stimulated 4 min after initiation of whole-cell recording either without (left panels) or with (right panels) 0.5 ng/μl $G_{\beta1\gamma2}$ subunits in the recording pipette. (**d**) Statistical analysis of **c**. (**e**) Secretion evoked by caffeine (20 mM, 10 s) was compared for cells stimulated 3 min after initiation of whole-cell recording either without (left panels) or with (right panels) 0.5 ng/ml $G_{\beta1\gamma2}$ subunits in the recording pipette. The same result was observed for ionomycin-induced secretion. (**f**) Statistical analysis of **e**.

Fig. 5 and **Fig. 6**). Taken together, these results support the idea that ATP inhibits secretion via $G_{\beta\gamma}$ subunits that directly interact with the fusion machinery in RACCs.

Opioids and somatostatin share the ATP inhibitory effect

In addition to ATP and its purinoceptors, chromaffin cells contain μ-opioid and somatostatin and their receptors, which inhibit I_{Ca} or catecholamine secretion[14,16]. Similar to ATP activation of P2Y receptors, both μ-opioid and somatostatin receptors are known to selectively activate $G_{i/o}$ signaling pathways[16,28,29,34]. We therefore asked whether activation of these receptors shares features of action with ATP. Our results indicated that activation of both receptors inhibited secretion by a mechanism that is shared with ATP receptor activation and is likely to involve similar G protein signaling systems (**Fig. 7**). Somatostatin reduced quantal size from 0.51 ± 0.04 pC to 0.25 ± 0.04 pC ($n = 14$) of that induced by caffeine but had no effect on quantal size of MCh-induced amperometric spikes (0.52 ± 0.05 pC to 0.50 ± 0.05 pC, $n = 8$, **Fig. 7a**). In addition, somatostatin inhibited 23 ± 2% ($n = 7$) of the I_{Ca} and 74 ± 9% (12.1 ± 2.2 pC versus 3.1 ± 1.1 pC, $n = 7$) of the depolarization-induced secretion. Somatostatin inhibited 48 ± 5% (11.4 ± 1.7 pC versus 5.9 ± 0.6 pC, $n = 12$) of the caffeine -induced secretion, 6 ± 4% (19.1± 4.2 pC versus 18.0 ± 0.7 pC, $n = 14$) of the MCh-induced secretion and 46 ± 7% (12.6 ± 2.2 pC versus 6.8 ± 0.8 pC, $n = 8$) of the MCh-induced secretion after pretreatment with 500 nM BIS (**Fig. 7c**).

DAMGO reduced quantal size from 0.52 ± 0.05 pC to 0.28 ± 0.04 pC ($n = 13$) of that induced by caffeine, but had no effect on quantal size of MCh-induced amperometric spikes (0.52 ± 0.05 pC versus 0.53 ± 0.04 pC, $n = 9$, **Fig. 7b**). In addition, DAMGO inhibited 25 ± 2% ($n = 8$) of I_{Ca} and 74 ± 8% (10.6 ± 2.1 pC versus 2.8 ± 0.8 pC, $n = 8$) of the depolarization-induced secretion. DAMGO inhibited 54 ± 6% (10.8 ± 2.0 pC versus 5.0 ± 0.6 pC, $n = 11$) of the caffeine-induced secretion, 3 ± 2% (21.2 ± 4.6 pC versus 20.6 ± 0.4 pC, $n = 13$) of the MCh-induced secretion and 44 ± 9% (11.4 ± 1.6 pC versus 6.4 ± 1.0 pC, $n = 9$) of the MCh-induced secretion after pretreatment with 500 nM BIS (**Fig. 7d**).

Endogenous PTX-sensitive $G_{i/o}$ inhibits quantal size

Having established that exogenous application of ATP, opioids or somatostatin reduces quantal size by means of activation of a PTX-sensitive $G_{i/o}$ pathway, we next tested whether endogenous transmitters released from a RACC would have a similar effect on quantal size. In order to avoid the effect of gap junctions between adjacent cells, we patch clamped an isolated cell (cell #1), and then lifted and placed it in contact with cell #2. A CFE was then placed on cell #1 for combined patch-clamp and amperometric recordings (**Fig. 8a**, right). In control recordings, cell #1 was depolarized for 1 s, triggering a burst of amperometric spikes (**Fig. 8a**, left). To test the possible effects of release of endogenous transmitters on cell #1, immediately before applying a second depolarizing pulse to cell #1, cell #2 was stimulated by local application of 70 mM KCl. Subsequent to stimulation of cell #2, the evoked transmitter release from cell #1 was smaller than the control, and, in particular, quantal size was reduced by 48 ± 1% (from 0.54 ± 0.04 pC to 0.26 ± 0.03 pC, $n = 12$). Finally, after recovery, the secretion evoked by the depolarizing step recovered to the control level.

It is likely that ATP, opioids or other endogenous ligands released from cell #2 activated $G_{i/o}$ pathways to cause inhibition in cell #1. This hypothesis was confirmed by the observation that incubation of chromaffin cell cultures with 250 ng/ml PTX for 24 h virtually abolished the reduction of quantal size (**Fig. 8b**). When pretreated with PTX, activating cell #2 resulted in a reduction of 5 ± 2% (from 0.54 ± 0.04 pC to 0.57 ± 0.04 pC, $n = 8$) of quantal size in cell #1. These data indicate that endogenous transmitters activate $G_{i/o}$ and reduce quantal size in RACCs (**Fig. 8c**).

DISCUSSION

ATP, opioids and somatostatin can each selectively activate a $G_{i/o}$ pathway in RACCs and inhibit secretion by two separate mechanisms:

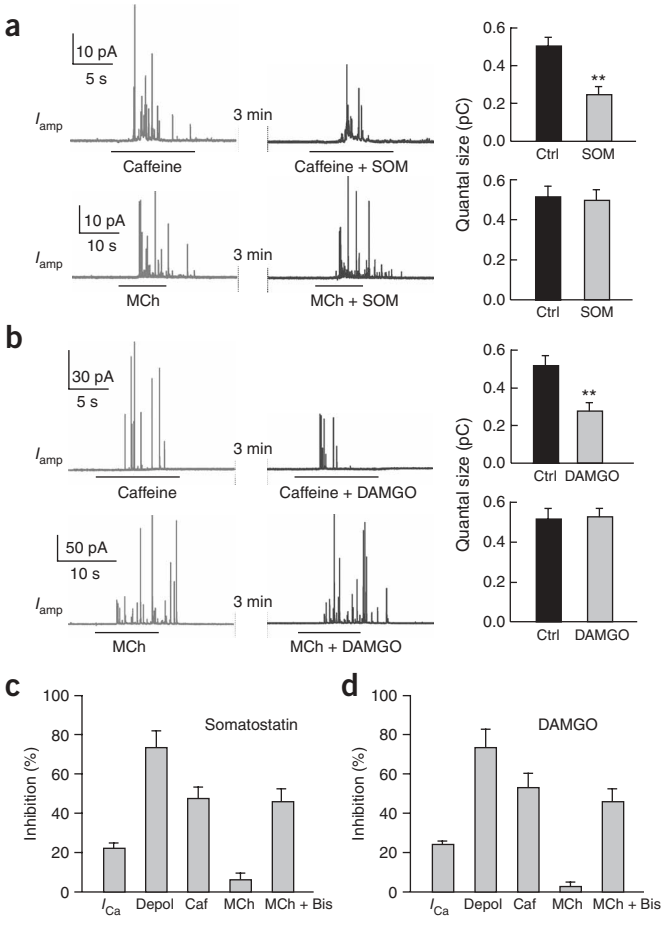

Figure 7 Somatostatin and the μ-receptor opioid, DAMGO, influence secretion in a manner similar to ATP. (**a**) Representative amperometric spikes induced by 20 mM caffeine (upper panels) or 100 μM MCh (lower panels) with or without 500 nM somatostatin (left panels). Histograms show the effect of somatostatin on quantal size evoked by caffeine (upper right) or MCh (lower right). (**b**) DAMGO (3 μM) inhibited secretion evoked by 20 mM caffeine (upper panels) but had no effect on secretion evoked by 100 μM MCh (lower panels). (**c**) Additional effects of somatostatin. Depol, depolarization. Caf, caffeine. (**d**) Additional effects of DAMGO.

inhibition of I_{Ca} and inhibition of the exocytotic machinery. Whereas stimulation of the receptor(s) inhibits about only 25% of the total I_{Ca}, depolarization-elicited secretion is inhibited by 80% (**Fig. 1a**; see also ref. 35). In bovine chromaffin cells, inhibition of I_{Ca} seems to account almost completely for inhibition of secretion by ATP[18,28,34]. Inhibition of I_{Ca} is thought to be the major mechanism for presynaptic inhibition[7]. However, the present results show that direct inhibition of the secretory machinery by a physiological $G_{i/o}$ pathway (~45%) may be of comparable importance to the inhibition of voltage-dependent Ca^{2+} channels (~55%) in RACCs (**Supplementary Fig. 5**).

$G_{\beta\gamma}$ subunits directly inhibit the secretory machinery

Scavenging of endogenous $G_{\beta\gamma}$ subunits by mSRIK, a membrane-permeable $G_{\beta\gamma}$-binding peptide[31,32], eliminated the ability of ATP to inhibit caffeine-evoked secretion. Although scavenging $G_{\beta\gamma}$ subunits may have other effects on cell function, the result implicates $G_{\beta\gamma}$ subunits in the ATP-induced effects. Furthermore, direct dialysis of $G_{\beta\gamma}$ subunits into RACCs mimicked the effect of ATP on secretion and amperometric spike kinetics.

$G_{\beta\gamma}$ subunits can modulate many cellular functions by a number of distinct effector pathways, including AC II, PI 3-kinase, PLC-β2 and several serine/threonine kinases and tyrosine kinases[8]. The failure of all of the tested compounds to block the ATP-mediated inhibition further supports the contention that a large number of signaling pathways are not involved in this effect.

In lamprey spinal cord synapses, injection of $G_{\beta\gamma}$ into presynaptic neurons inhibits neurotransmission downstream from presynaptic voltage-gated Ca^{2+} channels independently of $G_{\beta\gamma}$ -regulated cytoplasmic messengers[30]. Although this is consistent with a direct effect of $G_{\beta\gamma}$ on presynaptic vesicle-release proteins, it remains to be established whether this is also a general feature of secretory processes in mammals[36]. Furthermore, the mechanisms of the inhibitory effect (release probability or fusion pore kinetics) on the lamprey synapses by $G_{\beta\gamma}$ were unknown[30]. In the present work, we have demonstrated the mechanism that $G_{\beta\gamma}$ inhibits secretion by reducing the open time of the fusion pore in RACCs. Although we favor the idea that free $G_{\beta\gamma}$ directly regulates fusion pore open time, we cannot exclude the possibility that the apparent effect of $G_{\beta\gamma}$ could be caused by the whole G protein complex (G_{α} + $G_{\beta\gamma}$).

$G_{\beta\gamma}$ reduces the open time of the fusion pore

The reduction of quantal size resulting from the ATP inhibition and $G_{\beta\gamma}$ action might arise from either inhibiting the refilling of vesicles; or shortening the lifetime of the fusion pore. It seems unlikely that the acute application of ATP (co-puffed with caffeine) should lead to a rapid decrement in the average vesicle content. CFE measurements

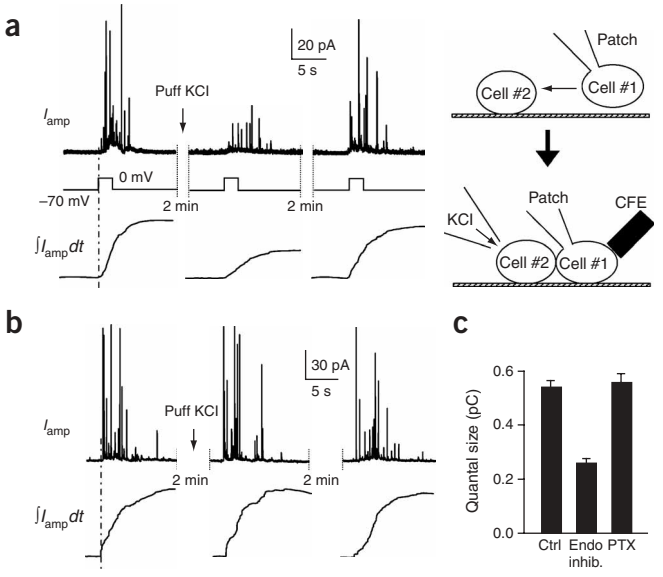

Figure 8 Endogenous reduction of quantal size by $G_{i/o}$ activation. (**a**) Activation of cell #2 by local application of 70 mM KCl reduced depolarization-induced secretion in cell #1 (left). Cell #1 was first patch clamped and then placed in contact with cell #2 (right). The depolarization pulse was applied to cell #1 during application of 70 mM KCl to cell #2. (**b**) After pretreatment of cells with 250 ng/ml PTX (24 h), depolarization-induced secretion in cell #1 was not inhibited by endogenous transmitter release from cell #2. (**c**) Effect of cell #2 activation on quantal size without and with PTX pretreatment.

showed that ATP reduces foot duration and foot charge (**Fig. 2**). Intracellular dialysis of $G_{\beta\gamma}$ subunits directly inhibited both quantal size and foot duration (**Fig. 6**). The foot in an amperometric spike is thought to reflect slow efflux of catecholamine through a fusion pore[3,12]. Therefore, the reduction in foot duration argues that fusion pore open time is reduced.

To further confirm that the ATP inhibition is by means of the fusion pore, we tested the role of dynamin in the ATP inhibition. Dynamin is a protein that is responsible for fission of endocytotic vesicles[4,21,22]. Intracellular dialysis of mutant dynamin (dynPRD), which had lost the GTPase activity necessary to close the fusion pore[21,23], increased fusion pore duration and eliminated the ATP effect on quantal size, HHD and foot duration (**Fig. 3**). Note, although dynamin affects the regeneration of endocytosed vesicles, it does not influence the parameters of amperometric spikes shown in **Figure 3**, because vesicle regeneration should affect only the total number of evoked amperometric spikes, but not the kinetics of single amperometric spikes (quantal size, HHD, foot duration, foot charge). Thus, these dynamin experiments provide additional evidence for the ATP effect on fusion pore opening.

Reversal of the $G_{i/o}$-mediated inhibition by PKC

We found that despite the robust inhibitory effects of ATP on both depolarization- and caffeine-evoked secretion, it had no effect on that induced by MCh. However, both bisindolylmaleimide and staurosporine treatment enabled ATP to inhibit the secretion evoked by MCh. Furthermore, treatment with PMA reversed the ATP-mediated inhibition of caffeine-induced secretion. These results argue that activation of PKC removes the ATP-induced inhibition of secretion in RACCs, although the mechanisms by which it does this are unknown.

In chromaffin cells, intensive stimulation facilitates secretion by means of activation of Ca^{2+}-dependent PKC[37]. PKC activation increases secretion strength by increasing the readily releasable pool and accumulating vesicle recruitment[9,26]. In the present work, we demonstrate another novel function of PKC activation; that PKC can remove the G_i-mediated inhibition of fusion pore opening. Future work should address the mechanisms by which PKC removes the ATP inhibition.

METHODS

Culture of chromaffin cells. Rat adrenal medulla chromaffin cells (RACCs) were prepared as described previously[15,38]. The use and care of animals in this study complied with the guidelines of the Animal Advisory Committee at the Shanghai Institutes for Biological Sciences.

$G_{\beta1\gamma2}$ peptide was a gift from C. He (Second Military Medical University, Shanghai)[33]. All other chemicals were from Sigma, except mSRIK, which was from Calbiochem.

Electrophysiological methods. Voltage-gated membrane currents were recorded using the nystatin perforated patch-clamp technique[38]. The holding potential was −70 mV and the cell was depolarized to 0 mV for 0.5–2 s to evoke secretion and current. For I_{Ca} recording, tetrodotoxin (100 nM) and TEA (20 mM) were used to inhibit the Na^+ and K^+ currents, respectively. In **Figure 8a,b**, as cell #1 was voltage-clamped at −70 mV, high KCl could not depolarize it, but it induced an inward (KCl) current of about −20 pA. Thus, there was no direct effect on secretion in cell #1 (data not shown).

A perfusion system (RCP-2B, INBIO) with a fast exchange time (<100 ms) for electronic switching between seven channels was used to change the external medium[39]. All experiments were carried out at room temperature (22–25 °C). Data are given as mean ± s.e.m. The significance of differences was determined using Student's *t*-test (*$P < 0.05$, **$P < 0.01$).

Electrochemical amperometry. Highly sensitive, low-noise, 5-μm carbon fiber electrodes (ProCFE, Dagan) were used for electrochemical monitoring of quantal release of catecholamines from single RACCs as described previously[3]. 'Foot' analysis was as described previously[3]. The onset of the foot was determined by a threshold of 5 s.d. above baseline, and the end of the foot was determined by the onset of the major spike (**Fig. 2b**). In all ATP application experiments, without preincubation, ATP was co-puffed with caffeine. For analysis of the kinetic properties of amperometric spikes, only events >5 s.d. were included. All the data were analyzed with Igor software (WaveMetrix) with a custom-made macro program[3].

$[Ca^{2+}]_i$ measurements. To estimate changes in intracellular Ca^{2+}, isolated RACCs were incubated for 15 min in a bath solution containing 2 mM Fura-2/AM (Molecular Probes) at 37 °C. Intracellular Ca^{2+} concentration $[Ca^{2+}]_i$ was measured by dual-wavelength ratiometric fluorometry. The Fura-2 was excited with light alternating between 340 and 380 nm using a monochromator-based system (TILL Photonics), and the resulting fluorescence signals were measured using a cooled CCD. Relative changes in $[Ca^{2+}]_i$ were calculated from the ratio of F_{340} to F_{380}, which were sampled at 1 Hz by fluorescence CCD imaging of a single cell[39]. The image data were transferred and analyzed by Igor software (WaveMetrix).

Note: Supplementary information is available on the Nature Neuroscience website.

ACKNOWLEDGMENTS

We thank C. He for the $G_{\beta1\gamma2}$ peptide, Y.T. Wang for the dynamin peptides and I. Bruce for reading the manuscript. This work was supported by grants from the National Basic Research Program of China (G2000077800 and 2006CB500800), the National Natural Science Foundation of China (30330210, 303328013 and C010505 to Z.Z.) and the US National Institutes of Health (DK46564 to C.L.).

COMPETING INTERESTS STATEMENT

The authors declare that they have no competing financial interests.

Received 18 May; accepted 28 July 2005
Published online at http://www.nature.com/natureneuroscience/

1. Ales, E. *et al.* High calcium concentrations shift the mode of exocytosis to the kiss-and-run mechanism. *Nat. Cell Biol.* **1**, 40–44 (1999).
2. Alvarez de Toledo, G., Fernandez-Chacon, R. & Fernandez, J.M. Release of secretory products during transient vesicle fusion. *Nature* **363**, 554–558 (1993).
3. Zhou, Z., Misler, S. & Chow, R.H. Rapid fluctuations in transmitter release from single vesicles in bovine adrenal chromaffin cells. *Biophys. J.* **70**, 1543–1552 (1996).
4. Elhamdani, A., Palfrey, H.C. & Artalejo, C.R. Quantal size is dependent on stimulation frequency and calcium entry in calf chromaffin cells. *Neuron* **31**, 819–830 (2001).
5. Wang, C.T. *et al.* Synaptotagmin modulation of fusion pore kinetics in regulated exocytosis of dense-core vesicles. *Science* **294**, 1111–1115 (2001).
6. Miller, R.J. Presynaptic receptors. *Annu. Rev. Pharmacol. Toxicol.* **38**, 201–227 (1998).
7. Wu, L.G. & Saggau, P. Presynaptic inhibition of elicited neurotransmitter release. *Trends Neurosci.* **20**, 204–212 (1997).
8. Hamm, H.E. The many faces of G protein signaling. *J. Biol. Chem.* **273**, 669–672 (1998).
9. Gillis, K.D., Mossner, R. & Neher, E. Protein kinase C enhances exocytosis from chromaffin cells by increasing the size of the readily releasable pool of secretory granules. *Neuron* **16**, 1209–1220 (1996).
10. Stevens, C.F. & Sullivan, J.M. Regulation of the readily releasable vesicle pool by protein kinase C. *Neuron* **21**, 885–893 (1998).
11. Sakaba, T. & Neher, E. Direct modulation of synaptic vesicle priming by GABA(B) receptor activation at a glutamatergic synapse. *Nature* **424**, 775–778 (2003).
12. Chow, R.H., von Ruden, L. & Neher, E. Delay in vesicle fusion revealed by electrochemical monitoring of single secretory events in adrenal chromaffin cells. *Nature* **356**, 60–63 (1992).
13. Zhou, Z. & Misler, S. Action potential-induced quantal secretion of catecholamines from rat adrenal chromaffin cells. *J. Biol. Chem.* **270**, 3498–3505 (1995).
14. Artalejo, A.R. Electrical properties of adrenal chromaffin cells. in *Electrophysiology of Neuroendocrine Cells* (eds. Scherubl, H. & Hescheler, J.) 259–294 (CRC, Boca Raton, Florida, 1995).
15. Neely, A. & Lingle, C.J. Effects of muscarine on single rat adrenal chromaffin cells. *J. Physiol. (Lond.)* **453**, 133–166 (1992).
16. Livett, B.G. & Boksa, P. Receptors and receptor modulation in cultured chromaffin cells. *Can. J. Physiol. Pharmacol.* **62**, 467–476 (1984).
17. Ennion, S.J., Powell, A.D. & Seward, E.P. Identification of the P2Y(12) receptor in nucleotide inhibition of exocytosis from bovine chromaffin cells. *Mol. Pharmacol.* **66**, 601–611 (2004).
18. Powell, A.D., Teschemacher, A.G. & Seward, E.P. P2Y purinoceptors inhibit exocytosis in adrenal chromaffin cells via modulation of voltage-operated calcium channels. *J. Neurosci.* **20**, 606–616 (2000).

19. Augustine, G.J. & Neher, E. Calcium requirements for secretion in bovine chromaffin cells. *J. Physiol. (Lond.)* **450**, 247–271 (1992).
20. Dodge, F.A., Jr. & Rahamimoff, R. Co-operative action a calcium ions in transmitter release at the neuromuscular junction. *J. Physiol. (Lond.)* **193**, 419–432 (1967).
21. Holroyd, P., Lang, T., Wenzel, D., De Camilli, P. & Jahn, R. Imaging direct, dynamin-dependent recapture of fusing secretory granules on plasma membrane lawns from PC12 cells. *Proc. Natl. Acad. Sci. USA* **99**, 16806–16811 (2002).
22. Graham, M.E., O'Callaghan, D.W., McMahon, H.T. & Burgoyne, R.D. Dynamin-dependent and dynamin-independent processes contribute to the regulation of single vesicle release kinetics and quantal size. *Proc. Natl. Acad. Sci. USA* **99**, 7124–7129 (2002).
23. Wang, Y.T. & Linden, D.J. Expression of cerebellar long-term depression requires postsynaptic clathrin-mediated endocytosis. *Neuron* **25**, 635–647 (2000).
24. Betz, A. *et al.* Munc13–1 is a presynaptic phorbol ester receptor that enhances neurotransmitter release. *Neuron* **21**, 123–136 (1998).
25. Rhee, J.S. *et al.* Beta phorbol ester- and diacylglycerol-induced augmentation of transmitter release is mediated by Munc13s and not by PKCs. *Cell* **108**, 121–133 (2002).
26. Nagy, G. *et al.* Protein kinase C-dependent phosphorylation of synaptosome-associated protein of 25 kDa at Ser187 potentiates vesicle recruitment. *J. Neurosci.* **22**, 9278–9286 (2002).
27. Graham, M.E., Fisher, R.J. & Burgoyne, R.D. Measurement of exocytosis by amperometry in adrenal chromaffin cells: effects of clostridial neurotoxins and activation of protein kinase C on fusion pore kinetics. *Biochimie* **82**, 469–479 (2000).
28. Currie, K.P. & Fox, A.P. ATP serves as a negative feedback inhibitor of voltage-gated Ca2+ channel currents in cultured bovine adrenal chromaffin cells. *Neuron* **16**, 1027–1036 (1996).
29. Neves, S.R., Ram, P.T. & Iyengar, R. G protein pathways. *Science* **296**, 1636–1639 (2002).
30. Blackmer, T. *et al.* G protein betagamma subunit-mediated presynaptic inhibition: regulation of exocytotic fusion downstream of Ca^{2+} entry. *Science* **292**, 293–297 (2001).
31. Goubaeva, F. *et al.* Stimulation of cellular signaling and G protein subunit dissociation by G protein betagamma subunit-binding peptides. *J. Biol. Chem.* **278**, 19634–19641 (2003).
32. Scott, J.K. *et al.* Evidence that a protein-protein interaction 'hot spot' on heterotrimeric G protein betagamma subunits is used for recognition of a subclass of effectors. *EMBO J.* **20**, 767–776 (2001).
33. He, C. *et al.* Identification of critical residues controlling G protein-gated inwardly rectifying K(+) channel activity through interactions with the beta gamma subunits of G proteins. *J. Biol. Chem.* **277**, 6088–6096 (2002).
34. Carabelli, V., Carra, I. & Carbone, E. Localized secretion of ATP and opioids revealed through single Ca^{2+} channel modulation in bovine chromaffin cells. *Neuron* **20**, 1255–1268 (1998).
35. Lim, W., Kim, S.J., Yan, H.D. & Kim, J. Ca^{2+}-channel-dependent and -independent inhibition of exocytosis by extracellular ATP in voltage-clamped rat adrenal chromaffin cells. *Pflugers Arch.* **435**, 34–42 (1997).
36. Jarvis, S.E. & Zamponi, G.W. Interactions between presynaptic Ca^{2+} channels, cytoplasmic messengers and proteins of the synaptic vesicle release complex. *Trends Pharmacol. Sci.* **22**, 519–525 (2001).
37. Smith, C. A persistent activity-dependent facilitation in chromaffin cells is caused by Ca2+ activation of protein kinase C. *J. Neurosci.* **19**, 589–598 (1999).
38. Duan, K., Yu, X., Zhang, C. & Zhou, Z. Control of secretion by temporal patterns of action potentials in adrenal chromaffin cells. *J. Neurosci.* **23**, 11235–11243 (2003).
39. Zhang, C. & Zhou, Z. Ca(2+)-independent but voltage-dependent secretion in mammalian dorsal root ganglion neurons. *Nat. Neurosci.* **5**, 425–430 (2002).